INT. J. NUM. METH. HEAT FLUID FLOW, VOL. 4, 367–377 (1994)

A NUMERICAL STUDY ON TURBULENT COUETTE FLOW AND HEAT TRANSFER IN CONCENTRIC ANNULI

S. TORII* AND W.-J. YANG**

* *Department of Mechanical Engineering, Kagoshima University, 1-21-40 Korimoto, Kagoshima 890, Japan*
** *Department of Mechanical Engineering and Applied Mechanics, University of Michigan, Ann Arbor, Michigan, 48109, USA*

ABSTRACT

A theoretical study is performed to investigate turbulent flow and heat transfer characteristics in a concentric annulus with a heated inner cylinder moving in the direction of flow (Couette flow). The two-equation k–ε model is employed to determine turbulent viscosity and kinetic energy. The Reynolds stress and turbulent heat flux are expressed by Boussinesq's approximation. The governing boundary-layer equations are discretized by means of a control volume finite-difference technique and numerically solved using a marching procedure. Results are obtained for the time-averaged streamwise velocity profile, turbulent kinetic energy profile, friction factor, and Nusselt number. These results agree well with experimental data in the existing literature. It is concluded from the study that the streamwise movement of the inner wall induces an attenuation in the turbulent kinetic energy, resulting in a reduction in the heat transfer performance and an increase in the velocity ratio of the moving inner cylinder to the fluid flow causes a substantial decrease in both the friction factor and the Nusselt number as well as a drastic reduction in the turbulent kinetic energy in the inner wall region.

KEY WORDS Turbulent Couette flow Moving core in concentric annuli Turbulent kinetic energy Friction factor Nusselt number

NOMENCLATURE

c_p	specific heat at constant pressure, J/kgK	q	heat flux, W/m^2
C_μ, C_1, C_2	empirical constants of k–ε model	r	radial coordinate, m
D	modification term in the wall region, in (7) or hydraulic diameter of the annulus, $2(R_{out}/R_{in})$, m	Re	Reynolds number
		R_{in}	inner radius of the annulus, m
		R_{out}	outer radius of the annulus, m
		R_t	turbulent Reynolds number, $k^2/\varepsilon\nu$
E	modification term in the wall region, in (8)	R_r	dimensionless distance in radial direction, y^+
f	friction factor	$\bar{T}$	time-averaged temperature, K
f_μ, f_1, f_2	turbulent model functions of k–ε model	T^+	dimensionless time-averaged temperature, $(\bar{T}_w - \bar{T})/(q_w/\rho c_p u^*)$
k	turbulent kinetic energy, m^2/s^2	t'	fluctuating temperature component, K
Nu	Nusselt number		
$\bar{P}$	time-averaged pressure,.Pa	U	velocity of a moving inner cylinder, m/s
Pr	Prandtl number		
Pr_t	turbulent Prandtl number	U^*	dimensionless relative velocity, U/u_m

0961–5539/94/040367–11$2.00

Received February 1993
Revised October 1994

u_m	axial mean velocity over tube cross section, m/s
$\bar{u}$, $\bar{v}$	time-averaged velocity components in axial and radial directions, m/s
u', v'	fluctuating velocity components in axial and radial directions, m/s
u^*	friction velocity, m/s
u^+	dimensionless velocity, $\bar{u}/u^*$
x	axial coordinate, m
y	distance from wall, m
y^+	dimensionless distance, u^*y/ν

Greek letters

ε	turbulent energy dissipation rate, m^2/s^3
α, α_t	molecular and turbulent thermal diffusivities, m^2/s
ν, ν_t	molecular and turbulent viscosities, m^2/s
λ	molecular thermal conductivity, W/mK
σ_k, σ_ε	turbulent Prandtl number for k and ε

Subscripts

b	bulk
in	inner side or inlet (Re)
max	maximum
w	wall
out	outer side

Superscripts

$-$	time-averaged value
$'$	fluctuation value

INTRODUCTION

The problem of heat and fluid flow in concentric annuli can be classified into three categories:

i) stationary cylinder case,
ii) parallel Couette flow case and
iii) circular Couette flow case.

Only turbulent flow will be considered here. The first category is encountered in various industrial applications, such as propulsion systems, heat exchangers and nuclear reactors, just to mention a few. Considerable efforts were directed at investigating turbulent transport phenomena in parallel flow through an annulus between two stationary concentric cylinders with a heated inner surface (for example, Brighton and Jones[1], Kays and Leung[2] and Heikal *et al.*[3]). The parallel Couette flow refers to a flow in a concentric annulus with one surface moving in the flow direction and the other remaining stationary (or both surfaces moving in the flow direction but at different velocities). The circular Couette flow corresponds to a flow with one surface rotating around the axis and the other remaining at rest (or both surface rotating in the same direction but at different angular velocities). Problems involving transport phenomena in both types of Couette flows can be found in many manufacturing processes such as extrusion, drawing, rolling and others.

Numerous studies were performed on various aspects of circular Couette flows, such as Taylor vortices, flow destabilization (for example, Schlichting[4]), heat transfer (for example, Kuzay and Scott[5,6]), and others.

In the parallel Couette flow case, Barrow and Pope[7] conducted a simple analysis simulating flow and heat transfer in railway tunnels (such as the 54-km long Seikan tunnel in Japan and the proposed English Channel tunnel). Recently, Shigechi *et al.*[8] obtained analytical solutions for friction factor and Nusselt number for turbulent fluid flow and heat transfer in concentric annuli with moving cores, using a modified mixing length model, originally proposed by van Driest[9]. It was disclosed that the friction factor is diminished while the Nusselt number is enhanced with an increase in the relative velocity (i.e. the velocity ratio of a moving inner core to the fluid flow). The conclusion contradicts that derived from the present numerical study utilizing the k–ε model. In another application, Lee and Kim[10] studied an inverted annular film boiling during an emergency core cooling of nuclear fuel channels which involved similar fluid flow and heat transfer phenomena.

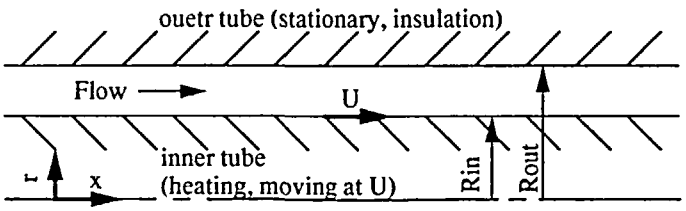

Figure 1 Physical system and coordinates

This paper treats turbulent flow and heat transfer characteristics in concentric annuli with the core moving in the flow direction. Emphasis is placed on the effects of core movement on friction factor and heat transfer rate. The two-equation k–ε model is employed to determine eddy viscosity. Numerical results are obtained by means of the control volume finite-difference technique.

GOVERNING EQUATIONS AND SOLUTION PROCEDURE

In the analysis of a turbulent annular flow in which a slightly heated inner cylinder moves in the flow direction, the governing equations for momentum and energy, by employing a cylindrical coordinate as depicted in *Figure 1* and the boundary layer approximations, can be expressed as:

$$\bar{u}\frac{\partial \bar{u}}{\partial x} + \bar{v}\frac{\partial \bar{u}}{\partial r} = -\frac{1}{\rho}\frac{\mathrm{d}\bar{P}}{\mathrm{d}x} + \frac{1}{r}\frac{\partial}{\partial r}\left(rv\frac{\partial \bar{u}}{\partial r} - r\overline{u'v'}\right) \tag{1}$$

$$\bar{u}\frac{\partial \bar{T}}{\partial x} + \bar{v}\frac{\partial \bar{T}}{\partial r} = \frac{1}{r}\frac{\partial}{\partial r}\left(r\alpha\frac{\partial \bar{T}}{\partial r} - r\overline{v't'}\right) \tag{2}$$

The Reynolds stress $-\overline{u'v'}$ and the turbulent heat flux $-\overline{v't'}$ in (1) and (2) are expressed through Boussinesq's approximation, as:

$$\overline{-u'v'} = \nu_t\frac{\partial \bar{u}}{\partial r} \tag{3}$$

$$\overline{-v't'} = \alpha_t\frac{\partial \bar{T}}{\partial r} \tag{4}$$

Here, the turbulent viscosity ν_t can be represented in terms of the turbulent kinetic energy k and its dissipation rate ε, according to Kolmogorov–Prandtl's relation as:

$$\nu_t = C_\mu f_\mu\frac{k^2}{\varepsilon} \tag{5}$$

where C_μ is an experimental constant. The turbulent thermal diffusivity α_t is obtained from the turbulent Prandtl number Pr_t as:

$$\alpha_t = \frac{\nu_t}{Pr_t} \tag{6}$$

$Pr_t = 0.9$ is employed in the present study. In order to evaluate k and ε in (5), a low Reynolds

number version of a k–ε turbulence model is used with transport equations of:

$$\bar{u}\frac{\partial k}{\partial x}+\bar{v}\frac{\partial k}{\partial r}=\frac{1}{r}\frac{\partial}{\partial r}\left\{r\left(\frac{\nu_t}{\sigma_k}+\nu\right)\frac{\partial k}{\partial r}\right\}+\nu_t\left(\frac{\partial \bar{u}}{\partial r}\right)^2-\varepsilon+D \tag{7}$$

$$\bar{u}\frac{\partial \varepsilon}{\partial x}+\bar{v}\frac{\partial \varepsilon}{\partial r}=\frac{1}{r}\frac{\partial}{\partial r}\left\{r\left(\frac{\nu_t}{\sigma_\varepsilon}+\nu\right)\frac{\partial \varepsilon}{\partial r}\right\}+C_1 f_1\frac{\varepsilon}{k}\nu_t\left(\frac{\partial \bar{u}}{\partial r}\right)^2-C_2 f_2\frac{\varepsilon^2}{k}+E \tag{8}$$

The k–ε models proposed by Jones and Launder[11], Nagano and Hishida[12], and Torii *et al.*[13] are employed in the present study. It is well known that these models, for ordinary wall turbulent shear flows, can predict the turbulence quantities such as Reynolds stress, turbulent kinetic energy and its dissipation rate in the vicinity of the wall as well as in the region far from the wall. The empirical constants and model functions in (5), (7) and (8) are summarized in *Table 1* for three turbulence models.

Boundary conditions for (1), (2), (7) and (8) are:

at $x = 0$ (start of heating):

hydrodynamically fully developed annular flow with a moving inner cylinder

at $r = R_{in}$ (inner tube wall):

$$\bar{u} = U \quad \text{(velocity of an inner cylinder)},$$

$$k = \varepsilon = 0,$$

$$-\frac{\partial \bar{T}}{\partial r}=\frac{q_w}{\lambda_w}$$

at $r = R_{out}$ (outer tube wall):

$$\bar{u} = k = \varepsilon = 0,$$

$$\frac{\partial \bar{T}}{\partial r} = 0 \quad \text{(insulation)}$$

No attempt is made to reduce the governing equations into dimensionless form, because no simplification is achieved by doing so. A control volume finite-difference technique, Patankar[14], is employed to discretize the governing equations. The resulting equations are solved from the inlet in the downstream direction by means of a marching procedure, since equations are parabolic. At each axial location, the pressure gradient $d\bar{P}/dx$ in (1) is corrected at every iteration in order to conserve the total flow rate. The procedure is repeated until a convergence criterion is satisfied. In the present study, the convergence criterion is set at:

$$\text{maximum}\left[\frac{\phi^M-\phi^{M-1}}{\phi_{\max}^{M-1}}\right]<1\times 10^{-4} \tag{9}$$

for all the variables ϕ ($\bar{u}$, $\bar{T}$, k, and ε). The superscripts M and $M-1$ in (9) indicate two successive iterations, while the subscript max refers to a maximum value over the entire fields of iterations. Nonuniform cross-stream grids are used in which the size is increased in a geometric ratio and the maximum is kept less than 3% of the hydrodynamic radius. The numbers of typical control volumes in the radial direction are 42 at Re = 10,000 and 69 at Re = 100,000. In order to ensure the accuracy of the calculated results, at least two control volumes are always located in the viscous sublayer. Throughout numerical calculations, the number of control volumes is properly selected between 42 and 92 to ensure validation of the numerical procedures and to obtain a grid-independent solutions. It results in no appreciable differences between the numerical

Table 1 Empirical constants and function for k–ε models

	Jones & Launder	Nagano & Hishida	Torii *et al.*
C_μ	0.09	0.09	0 09
C_1	1.45	1.45	1.44
C_2	2.0	1.9	1.9
σ_k	1.0	1.0	1.0
σ_ε	1.3	1.3	1.3
f_1	1.0	1.0	$1 + 0.28\exp\left(-\frac{R_t}{25}\right)$
f_2	$1 - 0.3\exp(-R_t^2)$	$1 - 0.3\exp(-R_t^2)$	$1 - 0.3\exp(-R_t^2)$
f_μ	$\exp\left\{\frac{-2.5}{1 + R_t/50}\right\}$	$\left\{1 - \exp\left(-\frac{R_t}{26.5}\right)\right\}^2$	$\left\{1 - \exp\left(-\frac{R_t}{26.5}\right)\right\}^2$
D	$-2\nu\left(\frac{\partial\sqrt{k}}{\partial r}\right)^2$	$-2\nu\left(\frac{\partial\sqrt{k}}{\partial r}\right)^2$	$-2\nu\left(\frac{\partial\sqrt{k}}{\partial r}\right)^2$
E	$2\nu\nu_t\left(\frac{\partial^2\bar{u}}{\partial r^2}\right)^2$	$\nu\nu_t(1 - f_\mu)\left(\frac{\partial^2\bar{u}}{\partial r^2}\right)^2$	$\nu\nu_t(1 - f_\mu)\left(\frac{\partial^2\bar{u}}{\partial r^2}\right)^2$

Table 2 Calculation conditions

Fluid	R_{in}/R_{out}	q_w (W/m²)	Re_{in}	U^*
			10000	
			20000	
			30000	0.0
Air	0.8	1000	40000	0.2
		2000	50000	0.4
			60000	0.6
	$R_{in} = 0.016$ m		70000	0.8
			80000	1.0
	$R_{out} = 0.020$ m		90000	
			100000	

results with different grid spacings. The calculation conditions are summarized in *Table 2*, including the Reynolds number, wall heat flux, relative velocity and tube size. It is necessary to verify all the three k–ε turbulence models employed here by comparing numerical predictions with experimental results for the flow field to determine the reliability of the computer code: The three models are applied to a flow in an annulus with a stationary, slightly heated inner cylinder. Numerical results are obtained at a location 220 tube diameter downstream from the inlet, where, thermally and hydrodynamically, fully developed conditions prevail. *Figure 2* depicts the distributions of the time-averaged streamwise velocity (dimensionless velocity u^+ *versus* y^+) at $Re = 46{,}000$. The results are compared with the universal wall law and the experimental results by Brighton and Jones[1]. Here *Figures 2(a)* and *(b)* correspond to the distributions from the inner and outer walls to the location of the maximum streamwise velocity, respectively. All the three models predict the velocity profile with the well-known characteristics of the logarithmic region. However, the models of Nagano and Hishida[12] and Torii *et al.*[13] yield a better agreement with the experimental data.

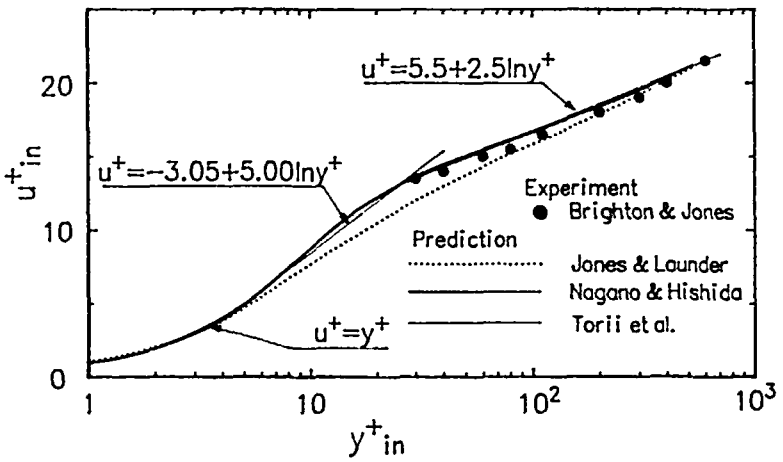

(a) inner side

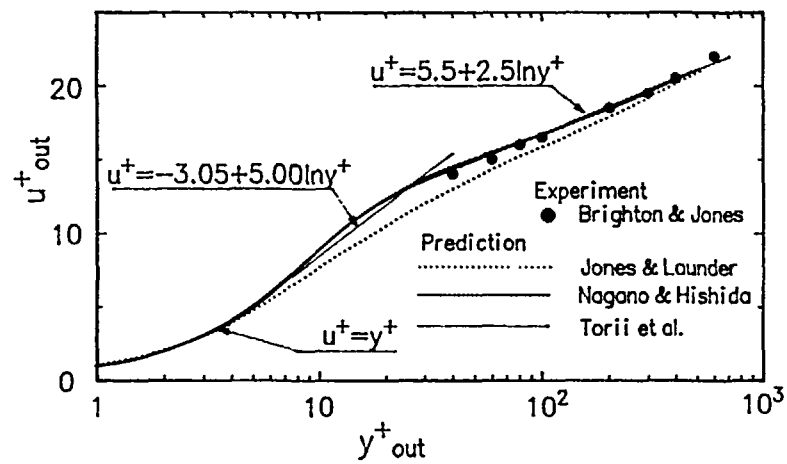

(b) outer side

Figure 2 Distribution of predicted time-averaged streamwise velocity in a stationary concentric annulus for $Re = 46{,}000$ and $R_{in}/R_{out} = 0.56$, (a) inner side and (b) outer side

Figure 3 shows the radial distribution of the calculated turbulent kinetic energy superimposed with the experimental data (Brighton and Jones[1]) at $Re = 46{,}000$. The predicted results by the three models are normalized by the square of the friction velocity $(u^*_{out})^2$ on the outer wall. Theory is in good agreement with the experimental results, but its accuracy is somewhat inferior near the inner wall than in the outer region.

Both the friction factor and the Nusselt number are presented in *Figure 4* as a function of the Reynolds number. Dalle Donne *et al.*[15] derived the following correlations for the Nusselt number and friction factor at the inner wall of the annulus as:

$$Nu_b = 0.0181\left(\frac{R_{out}}{R_{in}}\right)^{0.2} Re_b^{0.8} Pr_b^{0.4}\left(\frac{\bar{T}_{win}}{\bar{T}_{in}}\right)^{-0.18} \tag{10}$$

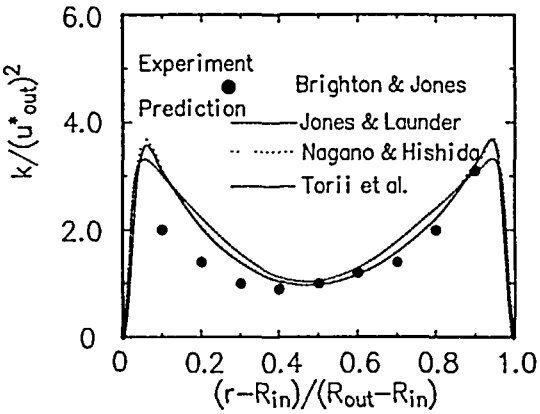

Figure 3 Distribution of predicted turbulent kinetic energy in a stationary concentric annulus for $Re = 46{,}000$ and $R_{in}/R_{out} = 0.56$

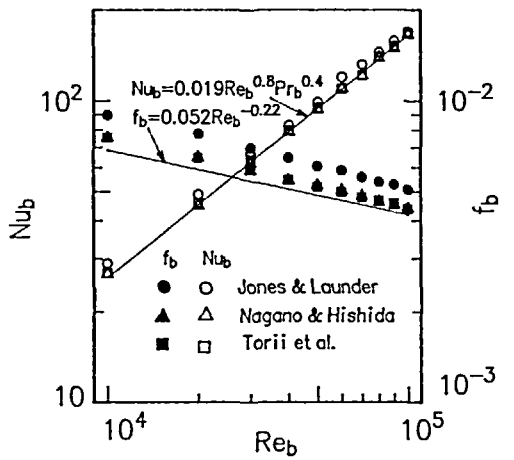

Figure 4 Predicted Nusselt number and friction factor in a stationary concentric annulus $R_{in}/R_{out} = 0.8$ and $x/D = 220$

$$f_b = 0.0615\left(\frac{R_{out}/R_{in}-1}{R_{out}/R_{in}}\right)^{0.1} Re_b^{-0.22} \tag{11}$$

The two equations are superimposed on *Figure 4* as solid lines. Note that *Figure 4* is under the temperature ratio of the inner wall to the fluid at the inlet, $\bar{T}_{win}/\bar{T}_{in}$, and the radial ratio, R_{in}/R_{out}, of 0.8. The calculated Nusselt number and friction factor are in good agreement with the correlation equations (10) and (11). It is observed that the Jones & Launder model slightly overestimates the flow and heat transfer performance than the other two models. The validity of the computer code and the accuracy for the three turbulence models are borne out through the above comparisons.

RESULTS AND DISCUSSION

Numerical results of the friction factor are illustrated in *Figure 5* with the velocity ratio of a moving inner cylinder to fluid flow, U^*, as the parameter. *Figures 5(a), (b), (c)* and *(d)* correspond

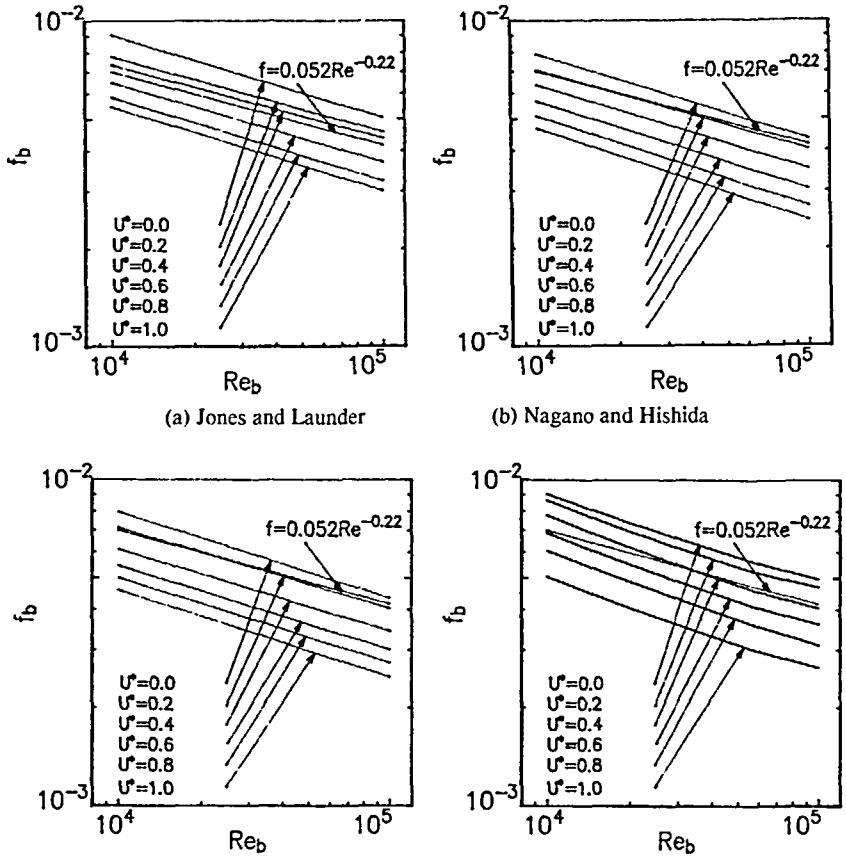

Figure 5 A comparison of predicted friction factors in a concentric annulus with a moving core for $R_{in}/R_{out} = 0.8$ and $x/D = 220$, using the k–ε models of (a) Jones and Launder, (b) Nagano and Hishida, (c) Torii *et al.*, and (d) analysis of Shigechi *et al.*

to the results obtained by the models of Jones and Launder[11], Nagano and Hishida[12], Torii *et al.*[13] and Shigechi *et al.*[8], respectively. It is observed in *Figures 5*(*a*), (*b*) and (*c*) that the friction factor diminishes with an increase in the dimensionless relative velocity. The same trend is seen in *Figure 5*(*d*). It is noted that the extent of reduction in the friction factor due to a change in the relative velocity is somewhat different for each model. The corresponding results of the predicted Nusselt number are illustrated in *Figures 6*(*a*), (*b*), (*c*) and (*d*), respectively. The effect of the relative velocity on the Nusselt number resembles that on the friction factor in *Figure 5*. An exception is the model of Shigechi *et al.*[8] which predicts an enhancement in the Nusselt number with an increase in the dimensionless relative velocity.

It is theorized that the substantial reduction in the Nusselt number observed in *Figure 6* is attributed to the core movement in the flow direction. In order to explain the mechanisms of these phenomena, numerical results for the streamwise velocity, turbulent kinetic energy and temperature at $Re = 10{,}000$ are obtained using the k–ε model of Torii *et al.*[13]. These results are presented in *Figures 7*, *8*, and *9*.

Figure 7 illustrates the radial profiles of the time-averaged streamwise velocity $\bar{u}/\bar{u}_{max}$ for different values of the dimensionless relative velocity, U^*. It is observed that as U^* is increased,

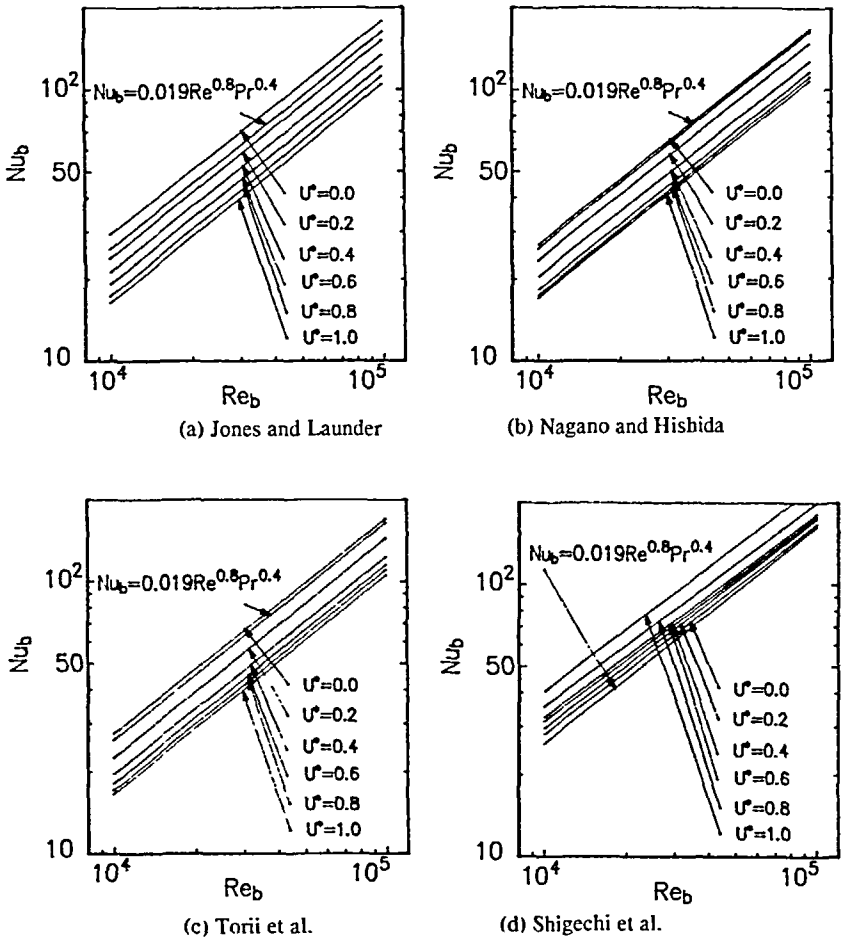

Figure 6 A comparison of predicted Nusselt numbers in a concentric annulus with a moving core for $R_{in}/R_{out} = 0.8$ and $x/D = 220$, using the k–ε models of (a) Jones and Launder, (b) Torii *et al.*, and (d) analysis of Shigechi *et al.*

the peak of $\bar{u}/\bar{u}_{max}$ shifts toward the inner side, resulting in a substantial deformation of the velocity of the fully developed turbulent annular flow from $U^* = 0$ for the stationary inner cylinder case. This implies that the velocity gradient at the inner wall is drastically reduced by the streamwise movement of the inner cylinder, with only a slight change in the outer wall region. The variation of the turbulent kinetic energy with a change in U^* is illustrated in *Figure 8*. One observes that the turbulent kinetic energy level in the inner wall region is also greatly reduced with an increase in U^*. In contrast, the turbulent kinetic energy in the central region increases somewhat, while no effect appears in the vicinity of the outer wall. This behaviour is in accord with the variation of the streamwise velocity $\bar{u}/\bar{u}_{max}$ in *Figure 7*. The radial profiles of the time-averaged temperature in the inner region T_{in}^+ are depicted in *Figure 9* for $U^* = 0$, 0.2, 0.4 and 0.6. Y^+ denotes the dimensionless distance from the heated wall. It is observed that the temperature distribution gradually approaches the laminar one ($T^+ = Pry^+$) as the relative velocity is increased.

In summary, a decrease in the Nusselt number, as seen in *Figure 6*, is certainly caused by the streamwise movement of the inner cylinder. This trend is amplified with an increase in the relative

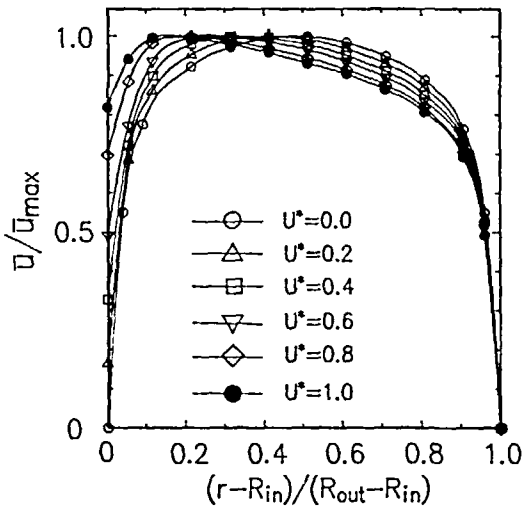

Figure 7 Variation of time-averaged streamwise velocity profiles with dimensionless relative velocity using the k–ε model of Torii *et al.* for $Re = 10{,}000$ and $R_{in}/R_{out} = 0.8$

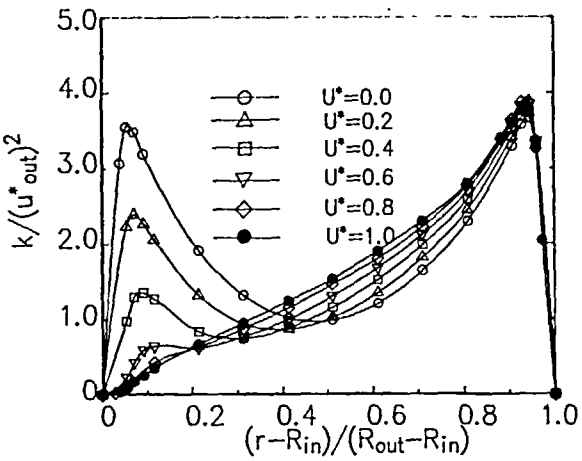

Figure 8 Variation of turbulent kinetic energy proviles with dimensionless relative velocity using the k–ε model of Torii *et al.* for $Re = 10{,}000$ and $R_{in}/R_{out} = 0.8$

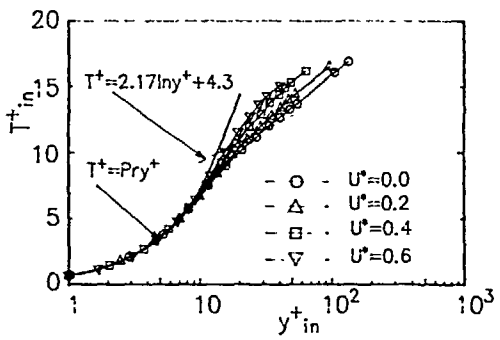

Figure 9 Variation of time-averaged temperature profiles with dimensionless relative velocity using the k–ε model of Torii *et al.* for $Re = 10{,}000$ and $R_{in}/R_{out} = 0.8$

velocity. The mechanism is that (i) in the region near the inner cylinder, a reduction in the velocity gradient induced by core movement suppresses that production of the turbulent kinetic energy, and (ii) it results in the deterioration of heat transfer performance.

CONCLUSIONS

Three existing k–ε models have been employed to numerically investigate the flow and heat transfer in concentric annulus with a slightly heated core moving in the flow direction. Consideration is given to the influence of relative velocity on the velocity and temperature distributions. The following conclusions are derived from the present study:

The k–ε models predict a reduction in both the friction factor and the Nusselt number with an increase in the relative velocity. Also disclosed are that the velocity gradient near the inner wall is decreased, the turbulent kinetic energy is substantially reduced in the inner region, and the radial profile of the time-averaged temperature gradually approaches the laminar one. Consequently, the turbulent kinetic energy in the region near the inner wall is substantially suppressed due to the streamwise movement of the inner cylinder, resulting in the deterioration of heat transfer performance.

REFERENCES

1 Brighton, J. A. and Jones, J. B. Fully developed turbulent flow in annuli, *Trans. of ASME*, **D**, 835–844 (1964)
2 Kays, W. M. and Leung, E. Y. Heat transfer in annular passages (hydrodynamically developed turbulent flow with arbitrarily prescribed heat flux), *Int. J. Heat Mass Transfer*, **6**, 537–557 (1963)
3 Heikal, M. R. F., Walkalate, P. J. and Hatton, A. P. The effect of free stream turbulence level on the flow and heat transfer in the entrance region of an annulus, *Int. J. Heat Mass Transfer*, **20**, 763–771 (1977)
4 Schlichting, H. *Boundary Layer Theory*, McGraw-Hill, New York (1968)
5 Kuzay, T. M. and Scott, C. J. Turbulent heat transfer studies in annulus with inner cylinder rotation, *ASME* Paper No. 75-WA/HT-55 (1975)
6 Kuzay, T. M. and Scott, C. J. Turbulent Prandtl numbers for fully developed rotating annular axial flow of air, *ASME* Paper No. 76-HT-36 (1976)
7 Barrow, H. and Pope, C. W. A simple analysis of flow and heat transfer in railway tunnels, *Heat Fluid Flow*, **8**, 119–123 (1987)
8 Shigechi, T., Kawae, N. and Lee, Y. Turbulent fluid flow and heat transfer in concentric annuli with moving cores, *Int. J. Heat Mass Transfer*, **33**, No. 9, 2029–2037 (1990)
9 van Driest, E. R. On turbulent flow near a wall, *J. Aerosp. Sci.*, **23**, 1007–1011 (1956)
10 Lee, Y. and Kim, K. H. Inverted annular film boiling, *Int. J. Multiphase Flow*, **13**, 345–355 (1987)
11 Jones, W. P. and Launder, B. E. The prediction of laminarization with a two-equation model of turbulence, *Int. J. Heat Mass Transfer*, **15**, 301–314 (1972)
12 Nagano, Y. and Hishida, M. Improved form of the k–ε model for wall turbulent shear flows, *Trans. ASME*, Ser D, **109**, 156–160 (1987)
13 Torii, S., Shimizu, A., Hasegawa, S. and Higasa, M. Laminarization of strongly heated gas flow in a circular tube (numerical analysis by means of a modified k–ε model), *JSME Int. J., Ser. II*, **33**, No. 3, 538–547 (1990)
14 Patankar, S. V. *Numerical Heat Transfer and Fluid Flow*, *Hemisphere, Washington, DC (1980)*
15 Dalle Donne, M. and Meerwald, E. Experimental local heat transfer and average friction coefficients for subsonic turbulent flow of air in an annulus at high temperatures, *Int. J. Heat Mass Transfer*, **9**, 1361–1376 (1966)